Article

Pitting Corrosion of Steel Pipes in Water Supply Systems: An Influence of Shell-like Layer

Valentin Chukhin [1], Alexey Andrianov [1] and Nikolay Makisha [2],*

[1] Department of Water Supply and Wastewater Treatment, Moscow State University of Civil Engineering, 26, Yaroslaskoye Highway, 129337 Moscow, Russia
[2] Research and Education Centre "Water Supply and Wastewater Treatment", Moscow State University of Civil Engineering, 26, Yaroslaskoye Highway, 129337 Moscow, Russia
* Correspondence: nmakisha@gmail.com

Abstract: The research was aimed at studying pitting corrosion, which precedes the appearance of fistulas in steel and cast-iron pipelines in water supply systems and leads to significant expenditures. The process of fistula formation is accompanied by the formation of tubercles and craters on the surface of a corroding metal. The study focused on examining the qualitative and quantitative composition of the solution, which is generated inside the tubercles during their growth. It was found that, during the operation of water pipelines, the concentration of aggressive chloride ions inside the tubercles increases significantly compared to the chloride content of the source water. The increase in chloride concentration leads to an accelerated corrosion rate, potentially causing the formation of fistulas over time. As a result of the study, a mechanism for changing the mineral composition of the solution inside the tubercles has been proposed. This is due to the manifestation of selective properties by a dense layer of tubercles. The study also examined the appearance of crystalline forms of corrosion products that form after removing pipes from the water supply system. The study also reveals the conditions of corrosion products emerging. Further studies on the structure and properties of a dense layer of corrosive sediment could be used to evaluate the effectiveness of various corrosion inhibitors.

Keywords: scale; pitting corrosion; steady water; steel and cast-iron pipes; tubercles; water distribution system

1. Introduction

The corrosion of steel pipelines in municipal water supply systems leads to significant economic losses. In particular, in the Russian Federation, over 1000 km of pipelines are completely replaced annually after decommissioning due to intensive corrosion. According to statistics, about 50% of the accidents and incidents in the field of housing and communal services are related to water supply, in particular to the gusts of water supply networks [1]. Accidents occur either due to a significant excess of the standard service life of pipelines or due to abnormally rapid corrosion, which develops in most cases unpredictably and has many causes [2–5]. Fistula on steel pipelines is the most common type of damage (68%).

The corrosion of steel pipes in cold and hot water supply systems has been quite well studied [3,6–8]. During operation, tubercles, which have a specific structure and composition, appear on the inner surface of pipelines. The structure of tubercles normally includes four elements: a loose surface layer; a thin but dense shell layer that creates a rigid framework of the tubercle; a loose core that includes corrosion products; and a corroding base [8–12]. Figures 1 and 2 show fragments of pipes with corrosive tubercles: the pipe with tubercles with a loose core (Figure 1) and the pipe with hollow tubercles (Figure 2). It was noted that the inner cavity of the tubercle is filled with an acidic solution [6].

Figure 1. A fragment of steel galvanized pipe with corrosion tubercles.
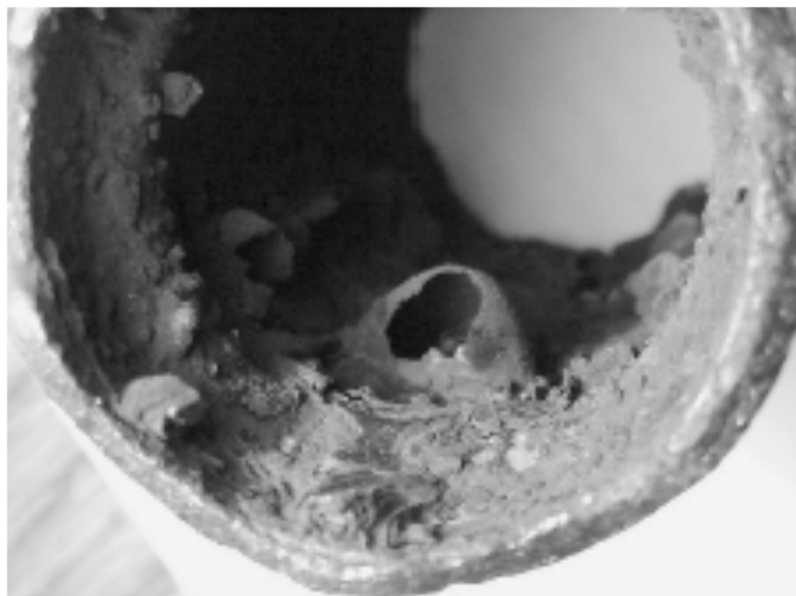
Figure 2. A fragment of steel pipe (from the fire-fighting water supply system) with corrosion tubercles [6].

The formation of the surface and shell layers of tubercles is quite well studied, as are the core structure and composition [8–13]. However, there are almost no studies that reveal the processes occurring inside the tubercles during their growth or experimentally prove the transition from ulcerative corrosion to pitting corrosion.

The study of the corrosion mechanism has three directions. The first direction is related to the effect of an external electric current on samples of various metals. This method includes electrochemical impedance spectroscopy (EIS). The second direction deals with the field studies of the corrosion of steel pipes, which are in operation. Finally, the third direction aims at the corrosion effects on pipelines that are no longer in service after an accident [14–16].

Most of the studies within the third direction are based on scale samples that are released from the environment of their formation. As a rule, it means a relatively long time from the sample extraction to their examination in the laboratory. This means that the accident consequences should be urgently localized; however, within this time, the scale structure undergoes significant changes [17].

Results of the structural and crystallographic composition of corrosive tubercles in a were presented in the research of Swietlik et al. [18]. These studies revealed the predominant presence of green rust, wherein iron compounds and various anions reflect the mineral composition of natural water. A significant amount of the least stable green rust in chloride form was found in almost all samples of the corrosive scale. During the experiment, the steady water that surrounds and partially fills the tubercles in the pipes was investigated. The study showed that drying the samples before analysis significantly changes the crystallographic phases in the corrosion products.

Table 1 shows the chemical composition of the steady water within the research of scale samples taken from cast-iron pipes of the water supply system with a diameter of 80–120 mm. The chloride content in the tap water sample was 130.8 mg/L, and the pH was 5.84 [18].

Table 1. The chemical composition of the steady water [18].

Cations [mg L^{-1}/meq L^{-1}]	Fe^{2+}	Mn^{2+}	K^+	Na^+	Mg^{2+}	Ca^{2+}
	960/32.28	3.5/0.064	3.8/0.097	23/1.0	12.6/1.036	170/8.5
Anions [mg L^{-1}/meq L^{-1}]	Cl^-	SO_4^{2-}	F^-	Br^-	NO_3^-	-
	1808.2/51.007	267.99/5.583	0.47/0.025	8.1/0.101	0.11/0.002	-

The total salinity was 3257.66 mg/L, and the concentration of chlorides in steady water was 13.8 times higher than the concentration of chlorides in the source tap water. The sum of the cations is 42.977 meq L^{-1}, and the sum of the anions is 56.718 meq L^{-1}. The inequality of the sums of anions and cations indicates that the steady water may contain other unaccounted cations. According to [19], the pH of the solution inside the pit should have a more acidic environment; therefore, a pH of 5.84 means that selected samples of steady water were partially diluted with the tap water. The undefined content of sulfates in the source water may be an indirect confirmation of the predominant chloride transfer.

In [19], the authors identified and studied two types of water: steady (near the tubercles) and occluded (inside the tubercles). The data on the chemical composition of both water types are generally consistent with the studies [20]. The authors also found a lower concentration of nitrates in steady water under stagnant conditions, which is explained by the reaction of nitrates with dissolved iron and the formation of nitrites and ammonium ions. The same effect was described in [21].

The above results of the steady water study reveal that the solution located inside the tubercles has a higher concentration than the water outside the tubercles. However, even within a short period between the extraction of the pipe and sampling, the concentration of salts in the steady water will decrease due to the dilution of the remaining water in the pipe. Therefore, the presence of high-concentration salts in the tubercles requires deep investigation, although the effect of water salinity on corrosion has been known for a long time [20,22,23]. The water composition is also important; the content of chlorides, sulfates, hardness, and alkalinity in the transported water affects the composition of corrosive deposits and the rate of iron release from the corrosive scale [24].

In the research of Soltis et al. [25] and Galvele et al. [26], the focus was on the sequence of pitting occurrence on stainless steel: the destruction of passivity, the emergence of pitting, and the pitting propagation. Two groups of pits are considered: metastable and stable. The difference between how these types of pits grow is that metastable growth ends with repassivation, whereas stable pitting continues growing. The development of a stable pit is determined by its internal chemical composition with a high concentration of salts.

Within the study of pitting corrosion on stainless steel samples [27], Pistorius and Burstein established the range of concentration values of the solution inside the pit, which precedes the growth of stable pitting. Research with stainless steel (type 304) showed that the concentration of metal cations in solution should be higher than 75–80% saturation of the chloride salt to prevent repassivation [28]. If the concentration of metal cations is less than about 75% saturation (i.e., below 3 M), the anolyte is not aggressive enough to support the rapid dissolution of the alloy, and repassivation is inevitable. The aggressive anolyte, which is formed in the growing pit, is the result of low pH and high chloride concentrations.

Based on the conducted research, Pistorius and Burstein proposed an equation by which the concentration of salts of corroding metal in pitting can be determined [27]:

$$\Delta C = \left(\frac{2\pi}{3 \times z \times F \times D} \right) \times i \times a \tag{1}$$

where ΔC is the concentration difference of metal cations between the inner surface of the pit and the bulk solution;

D is the diffusion coefficient of metal cations in solution;

i is the current density at which the pit is dissolving;

a is the pit radius;

F is the Faraday constant;

z is the oxidation state of the cations which are produced by dissolution.

Equation (1) shows that pit growth requires minimal values of multiplying current density i by depth or radius of pit a. If to apply that $\Delta C = 3$ M; $z = 2.19$; $F = 96{,}485$ C/mol; $D = 10^{-9}$ m^2/s, a critical value of $i \times a$ is equal to 0.3 A/m. The diffusion analysis determines a narrow range of $i \times a$ values in which the pit is stable. The lower limit requires that ΔC should exceed 3 M; the upper limit is determined by the solubility of the metal salt. If a saturation concentration of iron chloride is equal to 4.2 M, the condition for stable pit growth is expressed as:

$$0.3 \, \text{A} \cdot \text{m}^{-1} \leq i \times a \leq 0.6 \, \text{A} \cdot \text{m}^{-1} \tag{2}$$

A high concentration of salts in the pit can be explained by the pit size, which is small enough to neglect the effect of diffusion and convective transfer from the pit to the bulk solution. Moreover, the impact of the oxide film (partially preserved during the destruction) on the perforated coating has not been disclosed. This coating regulates the density of the corrosive current, providing an additional barrier to diffusivity.

In [29], Pistorius and Burstein clarified the role of the perforated coating, which "serves as an additional barrier to diffusion and maintains a sufficiently aggressive concentration of anolyte. Small breaks in this coating as the metastable pitting grows increase the diffusion rate without diluting the pitting anolyte and support the growth of the pitting. Such ruptures may occur due to the effect of the difference in osmotic pressure developing through the coating". In [30], Scheiner and Hellmich attempted to model the perforated coating and its effect on diffusion processes. The importance of coating was also highlighted in other studies [31,32]. In [33], the authors consider in detail the initial stage of pit nucleation and propagation. It was concluded that providing metastable pitting propagation requires a set of conditions to control diffusion: a current and surface roughness (the presence of occluded sites).

Research [34] is focused on the effect of chloride ions on pitting corrosion. It was shown that a concentration of chlorides of more than 245 mM in the electrolyte volume is required to maintain the spread of pitting on austenitic 316-L stainless steel. When chloride concentrations were below 245 mM, pitting became metastable.

Research [35] showed that the chloride ion creates an intermediate complex with a passive metal, followed by a sequential dissolution of the passive film and pit nucleation.

Some authors have noted the role of the solid salt film in the formation of pitting corrosion. The salt film can be formed on the metal surface because of the supersaturation conditions when the ionic concentration in the pit solution grows due to an increase in the

pit current density [36]. If a film exists, the rate of pit growth is limited by mass transport, and the pit has a regular hemispherical shape; if not, pits may have an irregular shape. Some studies reveal that the salt film helps to stabilize the pit and provide a buffer of ionic species, for example, in case of a sudden loss of a protective pit cover [37–39]. Additionally, salt film promotes oxide passivation in solutions that contain perchloric and sulfuric acids at potentials above the passivation potential [39].

Numerous publications were aimed at factors that affect the corrosion potential and their importance for the initiation of pitting and overall corrosion [23,40,41]. During stagnation, the corrosion potential of iron decreases noticeably [40].

Despite the quite comprehensive knowledge about the mechanism of pitting corrosion, it should be noted that in the above works, the research was carried out with highly concentrated solutions. However, these studies did not disclose how these concentrations of salts were created at the metal-solution boundary within the tap water with a lower salinity. Therefore, the main purpose of current research is to clarify the mechanism of the implementation of suitable conditions for the occurrence and development of pitting corrosion.

2. Materials and Methods

Dried scale samples from old corroded steel pipes were examined in the current research. The study was based on the investigation of the effect of electrolyte concentration on pitting corrosion. It was supposed that a shell-like layer provides an exchange between internal and external media [9,42], and consequently, the liquid fraction of the scale inside the tubercles can be extracted by repeated dissolution and analyzed.

The experiment consisted of extracting tubercles from defective pipes and analyzing soluble scale components of tubercles after the pipelines were taken out of service. At the same time, the anionic composition was focused on because during drying, iron cations are oxidized to form insoluble substances deposited in the structure of the tubercles. It allows for analyzing the processes inside the pipe even if the study was carried out after a long period from the pipe extraction from the distribution network.

Studies of the structural features of the tubercles were carried out on the pipes after being in operation. The inner surface of a fragment of an uncoated steel pipe DN 300, extracted from the water supply system in Moscow, is shown in Figure 3. Corrosion deposits on the surface of the pipe are solid, dense, and durable, with oval tubercles measuring from 5×5 to 10×10 mm and with a height of 5–8 mm. The pipe service life was 36 years. The tubercles were divided into three groups according to the following criteria. Tubercles with a full set of structural differences were assigned to Group 1: surface layer, shell layer, core, and base. The second group of tubercules was without a base, and the third group included the most deformed tubercules removed from the pipe. Figures 3 and 4 show photographs of the inner surface of the pipe.

The surface of the pipe under the layer of corrosive deposits has traces of entire ulcerative corrosion and spot damage on the background of flat traces. The depth of spot damage was from 1.0 to 3.0 mm, and the diameter was from 2 to 5 mm. There are also traces of extensive corrosion; the thickness of the corroded metal can be estimated from the remaining sections at 0.5–1.0 mm.

The content of chlorides, calcium, and magnesium was determined by titration with standard solutions. Iron, sulfates, and nitrates were measured on a Lange 5000 spectrophotometer (Hach, Loveland, CO, USA), and pH was measured with a Hanna HI 2215 pH meter (Hanna Instruments, Woonsocket, RI, USA). Micrographs of the scale were made on a Quanta FEI 250 electron microscope (FEI Company, Hillsboro, OR, USA) in the mode of secondary electrons without coating at an accelerating voltage of 10–25 kV.

Figure 3. Inner surface of the pipe (d = 300 mm, carbon steel).
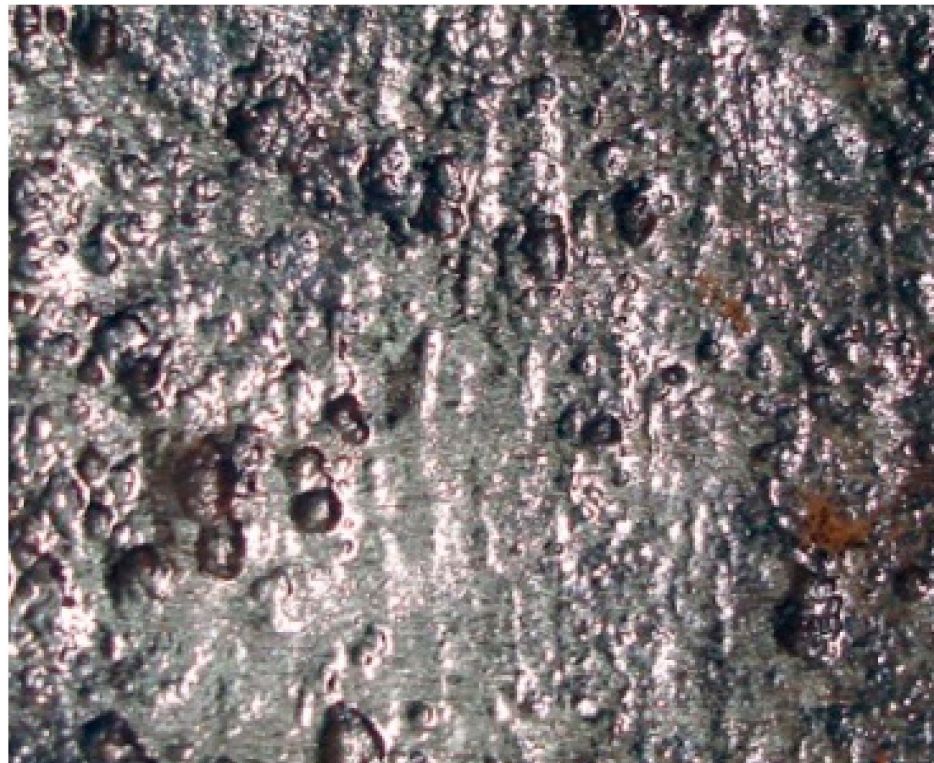
Figure 4. Photo of the pipe inner surface after removal of corrosion deposit layer (zoom 2x).

3. Results and Discussion

The experiment was performed in the following sequence. The suspended particles of the tubercles with the removed pulverized fractions were placed in a measuring cylinder with a fixed volume of distilled water (V_1), and the volume of water displaced by the scale (V_2) was immediately measured. Then, a change in the volume of water (V_3) absorbed by tubercles was observed within the next 48 h. According to these data, the density of the tubercle material was calculated, as was the volume of water ($V_4 = V_2 - V_3$) in the scale

at the time of extraction from the cylinder. The concentration factor K was determined as $K = V_1/V_4$. Table 2 shows the values of scale density and the amount of absorbed water.

Table 2. Scale sorption of distilled water.

| Sample | Scale Mass [g] | Volume of Distilled Water [mL] | | | | Concentration Factor, K | Scale Density [g cm^{-3}] |
		Without Scale, V_1	With Scale, V_2	After 48 h, V_3	Absorbed by a Scale, V_4		
1	50.4095	150	173	170	3	50	2.52
2	50.2405	150	171	167.5	3.5	42.8	2.87
3	50.2026	150	172	168.5	3.5	42.8	2.71

During the study, it was assumed that V_4 was equal to the volume of the solution that was in the tubercles before the removal of the pipe. Distilled water, penetrating into the pores, desorbs well-soluble salts located inside the tubercles and forms a mixed solution of salts. Thus, after 48 h, the concentration of salts in the cylinder and in the tubercles is equalized. The relatively low scale density (2.65–2.87 g/cm^3) compared with the density of iron oxides and hydroxides indicates the presence of pores and voids in the structure of the tubercles.

The values of ion concentrations in the solution inside the tubercles were determined by multiplying the concentration of salts in the water sample after desorption and dissolution of salts from the tubercles by the concentration factor K (Table 3). Desorption of salts from the tubercles was carried out once.

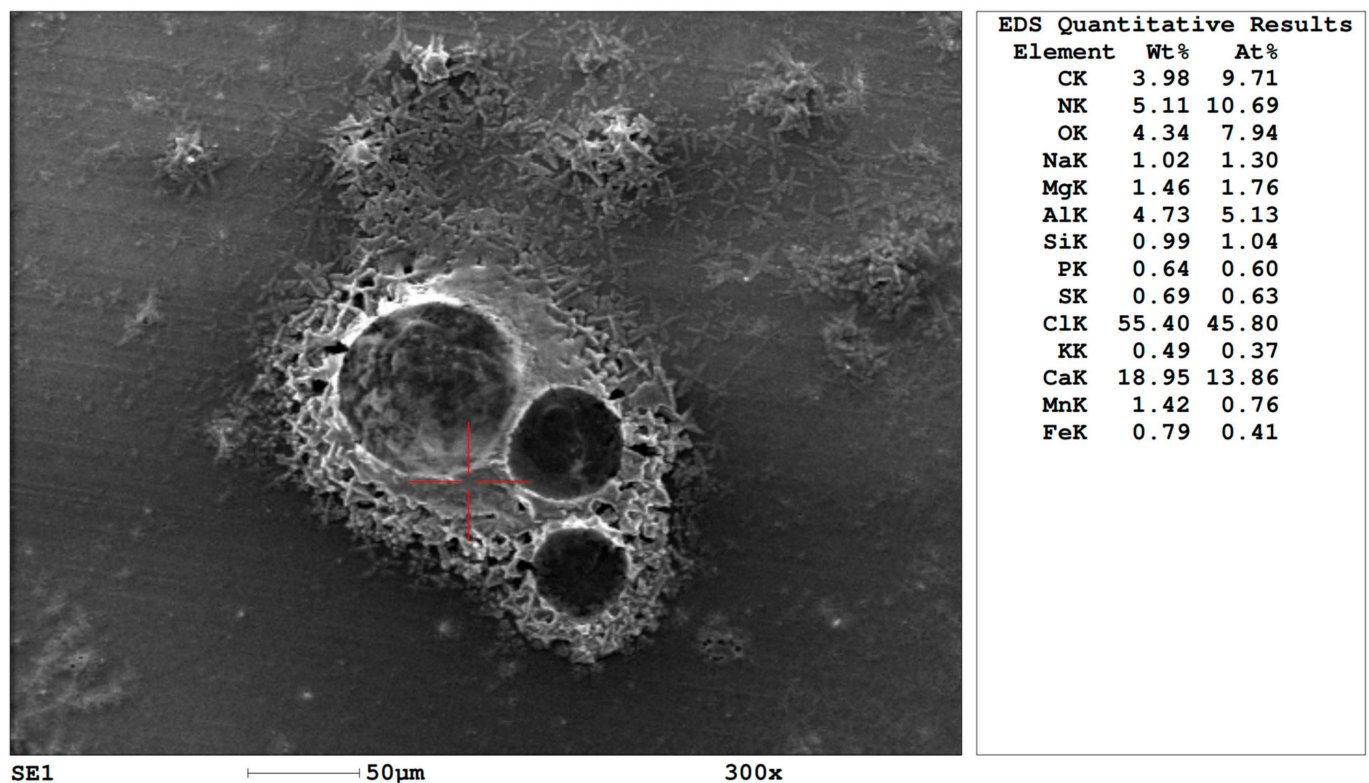**Table 3.** Estimated composition of the solution inside the tubercules.

| Sample | pH */** | Concentration [meq/L] | | | | | | |
		H^+	Cl^-	SO_4^{2-}	NO_3^-	Fe^{2+}	Mg^{2+}	Ca^{2+}
1	3.32/1.63	23.93	756	1.0	0.24	5.05	150	550
2	3.73/2.10	7.97	647	0	0.83	3.59	171	471
3	3.28/1.65	22.46	749	0	0.97	5.91	170	514

Note: * determination of water with desorbed salts in a sample; ** calculated value.

According to the acidity of each sample and the concentration factor, the pH values of solutions in the pores of the tubercles were calculated at the time when pipeline operation was stopped. These values were 1.63, 2.10, and 1.65, respectively.

The results in Table 3 confirm that the tubercle within its growth contains a multi-component salt solution. The total concentration of salts inside the tubercle significantly exceeds the salt content in the source water in the pipeline. If the chloride content in the composition of the internal solution was predictable, the high content of magnesium and calcium was unexpected.

In addition to determining the composition of water, the qualitative composition of desorbed salts was evaluated. For this purpose, 3 mL of water was evaporated on an aluminum foil substrate in a drying cabinet at a temperature of 80 °C. The dry sediment was studied using a Quanta FEI 250 scanning electron microscope and an EDAX (Gatan, Pleasanton, CA, USA) energy dispersion spectral analyzer (Figure 5).

EDS Quantitative Results

Element	Wt%	At%
CK	3.98	9.71
NK	5.11	10.69
OK	4.34	7.94
NaK	1.02	1.30
MgK	1.46	1.76
AlK	4.73	5.13
SiK	0.99	1.04
PK	0.64	0.60
SK	0.69	0.63
ClK	55.40	45.80
KK	0.49	0.37
CaK	18.95	13.86
MnK	1.42	0.76
FeK	0.79	0.41

SE1   50μm   300x

Figure 5. Spectrogram of the elemental composition (in the area marked by a red cross) of desorbed water.

The data obtained using the electron microscope show that the main components of the solution are chlorides, nitrates, and calcium. The contribution of each of the other elements is estimated at 0.3–1.5%. The acidic medium of the solution is determined by the presence of hydrogen cations.

The analysis of the obtained results, based on the structural features of the tubercles and theoretical aspects of corrosion, allows for the description of the development of pitting corrosion inside water pipes. The formation of tubercles goes with the first phase, which involves fixing the base of the tubercle on the inner surface of the pipe and forming a dense layer firmly adjacent to the metal. In [43,44], it was observed that the contour of the tubercle on the metal surface is formed by the water flow in the pipe and fixed after 60–70 days. Anodic and cathodic areas appear on the metal surface; afterward, a loose layer of iron hydroxides with immobilized water grows on the anode sites. The corrosion process is controlled by oxygen depolarization. As the oxygen concentration on the metal surface decreases, the redox environment changes inside the scale layer, which is followed by the formation of a dense layer and the tubercle [15]. The dense layer at this stage is relatively permeable to ions and water. The conversion of iron hydroxides into magnetite, which forms a dense layer, proceeds with the dehydration of hydroxides and leads to the appearance of free water inside the tubercle. In the absence of oxygen, hydrogen ions act as the depolarizer. Hydrogen ions are reduced to molecular hydrogen at the cathode sites of the metal inside the tubercle, forming "chimneys" in the structure of the tubercle [44]. The medium inside the tubercle is acidified due to the reaction of Fe^{2+} hydrolysis.

The second phase includes an increase in salt concentration inside the tubercle. According to the previous research results [27,28], the pit is stable at a very high solution concentration of approximately 3 mol/L. Thus, it is necessary to explain how a dense layer provides not only the transfer of ions and water but also ensures the appearance of a solution with a high concentration. A well-studied method for obtaining highly concentrated solutions under the action of electric current is electrodialysis. As a rule, devices with "closed" brine chambers with no external water supply can be applied, while the

concentration occurs due to osmotic and electroosmotic transfer of hydrated ions through selectively permeable anion-exchange and cation-exchange membranes [44].

Since metal serves as an anode for corrosion, anions are required to neutralize the charge of iron cations. Therefore, the dense layer should act as an anion-exchange membrane. Based on the studies of the qualitative composition of desorbed salts, it can be stated that the dense layer has selective properties, preferably passing monovalent chloride ions (Table 3). Thus, an increase in the concentration of iron cations inside the tubercle (because of corrosion) is provided by the transfer of an equivalent amount of hydrated chloride ions (as well as sulfates and nitrates), leading to an increase in the total concentration of the electrolyte and an increase in its aggressive properties.

From the theory of electrodialysis, it is known that the concentration of fixed ions in the membrane structure limits the maximum concentration of brine on electrodialysis devices [45,46]. It was experimentally established that the concentration of the salt solution, which can be achieved during membrane concentration, grows within the increase of current density and membrane selectivity. This corresponds to the studies of Pistorius and Burstein on the dependence between the electrolyte concentration inside the pit and the current density [27].

It can be assumed that the high concentration of the solution in the tubercle is also associated with the concentration of fixed charges in the dense layer. Fixed ions are embedded in the voids of the crystal lattice of a dense layer that occurs during its formation. At the same time, the high concentration of fixed cations in the dense layer prevents the access of iron ions into the water flow outside the tubercle. Thus, the total concentration of electrolyte in the structure of the tubercle can reach high values, as follows from the data in Table 3.

Obviously, the permeability of a dense layer is developed within its formation during the transfer of hydrated anions to a soluble anode. At the same time, the pressure inside the tubercle increases due to the electroosmotic transfer of water, contributing to the dense layer growth and, in some cases, its destruction.

The anion selectivity of the dense layer can be confirmed based on the comparison of the quality of the water sample with desorbed salts and the water sample in the water supply system during pipe operation. For example, in Moscow, chloride content in tap water is no more than 10% of the total anionic composition, while chloride content in desorbed salts exceeds 99%. According to the above, the selective properties in a dense layer can be confirmed by the concentration of chloride ions in the desorbed solution and the inhibitory effect of individual anions on the potential of pitting formation. Overall, corrosion rate can be influenced by introducing various inhibitors [29,47,48].

The third phase includes the processes preceding the formation of a fistula. This stage can be represented as a complex effect on the metal surface of a multitude of pits that form on a limited metal surface directly under a dense layer of tubercle. At this stage, the tubercle stops growing and goes into the mode of autocatalytic action. The corrosion inside the tubercle intensifies as the metal is now in contact with a concentrated solution of $FeCl_2$ instead of tap water. Corrosion is supported mainly by water, which is located directly in the volume of the tubercle.

At the last stage, the role of hydrolysis of iron chloride with the formation of H^+ and OH^- ions should be noted. They inhibit the growth of iron concentration, creating crystalline forms of $Fe(OH)_n$. On the other hand, the reduction of H+ ions to hydrogen gas at the cathode contributes to sealing the pores of a dense layer due to the large size of gas bubbles, which exceed the pore size. Thus, the condition for the fistula emerging is an amount of water within the tubercle core that is sufficient for the oxidation of iron ions, considering the remaining thickness of metal. In case of a shortage of water, separate pits and the overall tubercle are repassivated. Therefore, pipes with a thicker wall (cast iron pipes, for instance) are more resistant to corrosion.

When analyzing damage to the pipe walls caused by fistulas, attention should be paid to the formation of a conical crater on the inner wall of the pipe, with a pit in the crater

center. If the high concentration of chlorides causes the formation of a fistula, the presence of the hollows on the walls of this crater may be expected, eventually reaching the outer boundary of the pipe wall and forming a fistula. However, the analysis of the crater surface did not confirm such expectations. That means that in addition to the effects that chlorides have, other anions also participate in corrosion. This is confirmed by the study [49], which presents the research on the corrosion of 304 stainless steel in seawater. The results of experiments and simulations show that Cl^- corrodes locally with the formation of narrow and deep pits, while Br^- has a polishing effect, forming shallow and wide pits.

Figures 1 and 2 reveal photographs of pipes with different tubercle structures. Since the corrosion in the formed tubercle occurs in an area bound by the contour of the tubercle, iron accumulates inside the tubercle. At the same time, favorable conditions occur for the precipitation of iron oxides, which have low solubility. Figure 6 shows the sizes of crystal structures that can be used to calculate the density of the corrosive current according to Equation (2).


(**a**)

(**b**)

(**c**)

(**d**)
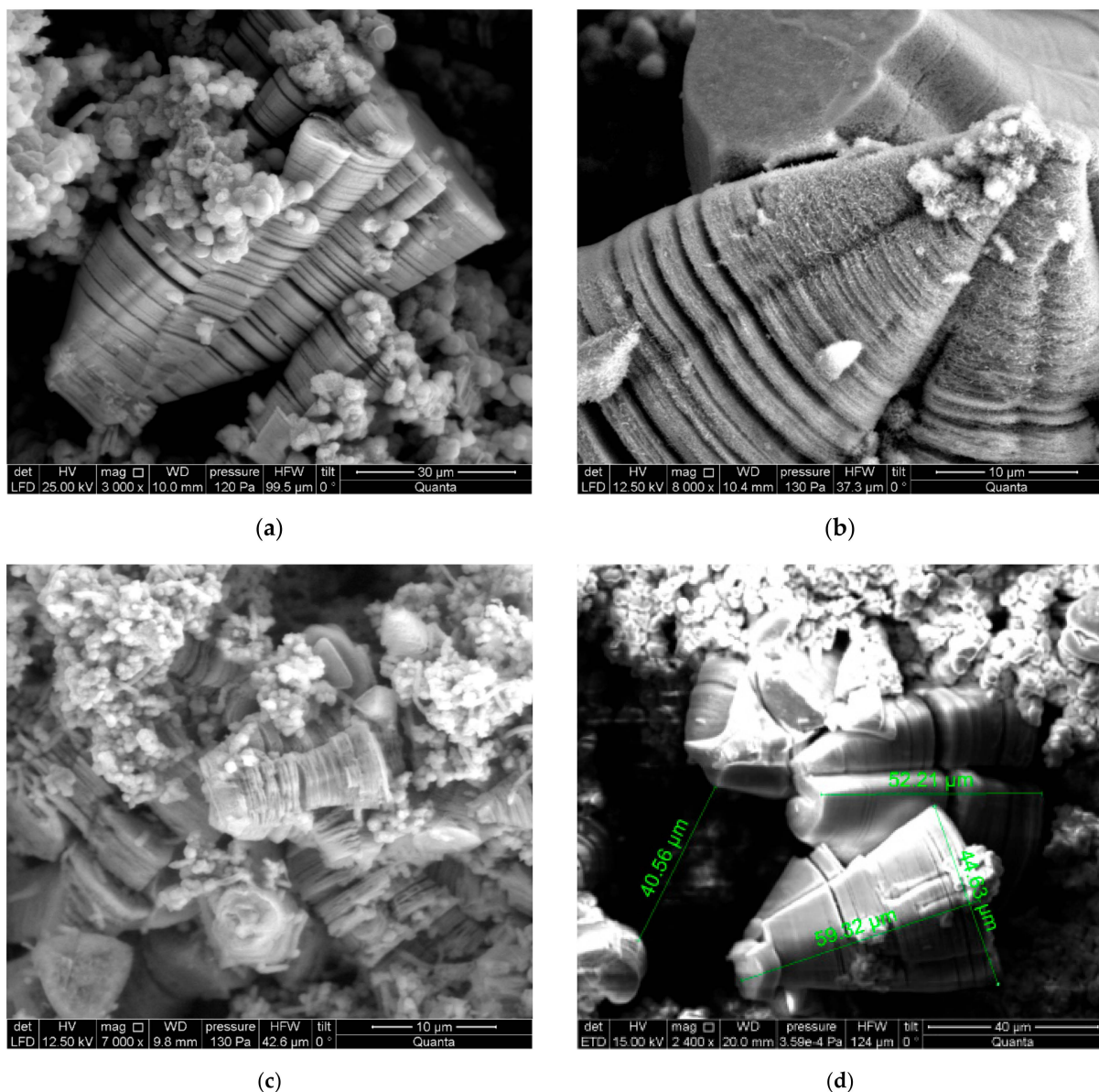
Figure 6. Forms of scale in steel pipes within fistulas formation under different magnification: (**a**) 3000×; (**b**) 8000×; (**c**) 7000×; (**d**) 2400×.

Figure 6 shows photographs that explain the last stage of the development of pitting corrosion. The metal under the tubercle collapses and forms crystalline conical structures, which duplicate the shape of the pitting. This happens due to the lack of water inflow into the tubercles through a dense layer or a limited amount of water in the pitting structure.

Figure 6 shows the formation of a large number of conical elements. The chaotic location of separate crystals indicates the mutual movement of crystal structures inside the core of the tubercle with continued corrosion. If the volume of water is sufficient inside the tubercle, then the shallow pit can turn into a deep one. Otherwise, the corrosion may stop completely or be suspended for a while in accordance with external conditions. Crystal structures fill the inner volume of the tubercle during the entire life of the pipeline; therefore, the presence of dense tubercles is characteristic of pipes that have been in operation for a long time.

Additional information about the process of scale formation in pipes can be provided by the analysis of photographs obtained after the extraction of tubercles. Figure 7 shows micrographs of corrosion scales removed from an uncoated steel pipe of the cold water supply system DN 900 mm (a) and a galvanized steel pipe DN 100 from the hot water supply system (b).
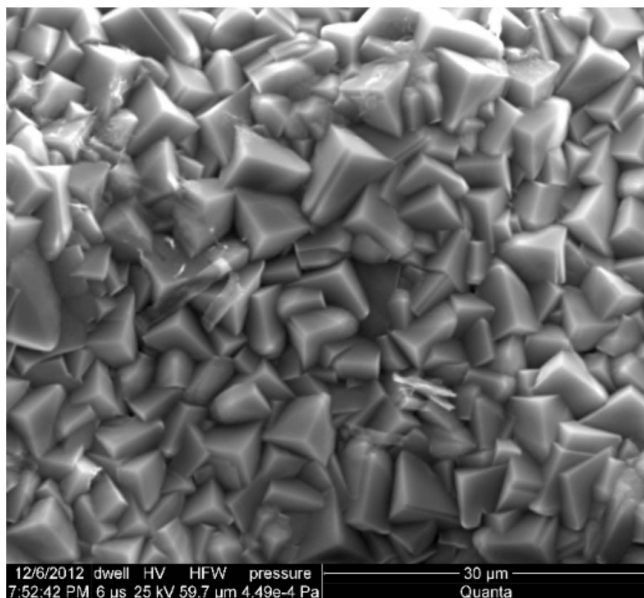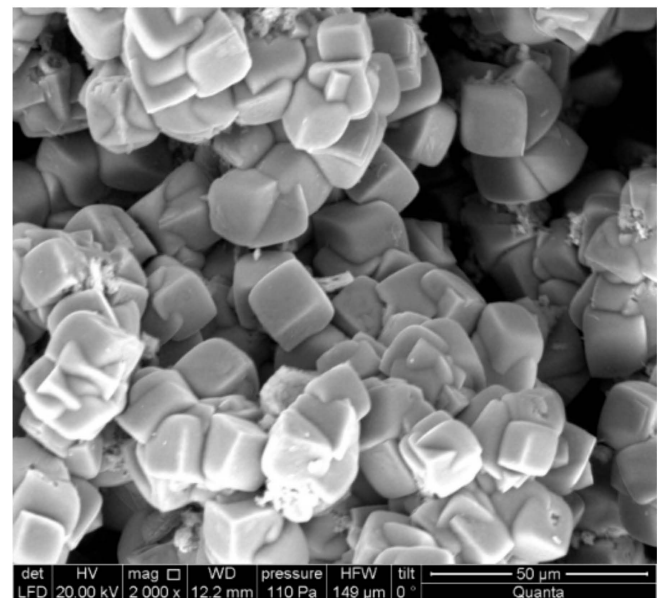

(**a**) (**b**)

Figure 7. Microphotographs of corrosion scales in cold water pipes (**a**) and hot water pipes (**b**).

Hemispherical scale crystals, which copy the metal surface, are formed with a significant oversaturation of the solution. The second condition is the absence of spatial restrictions confirming the presence of a high concentration of iron salts in the inner volume of the tubercles (Figure 8).
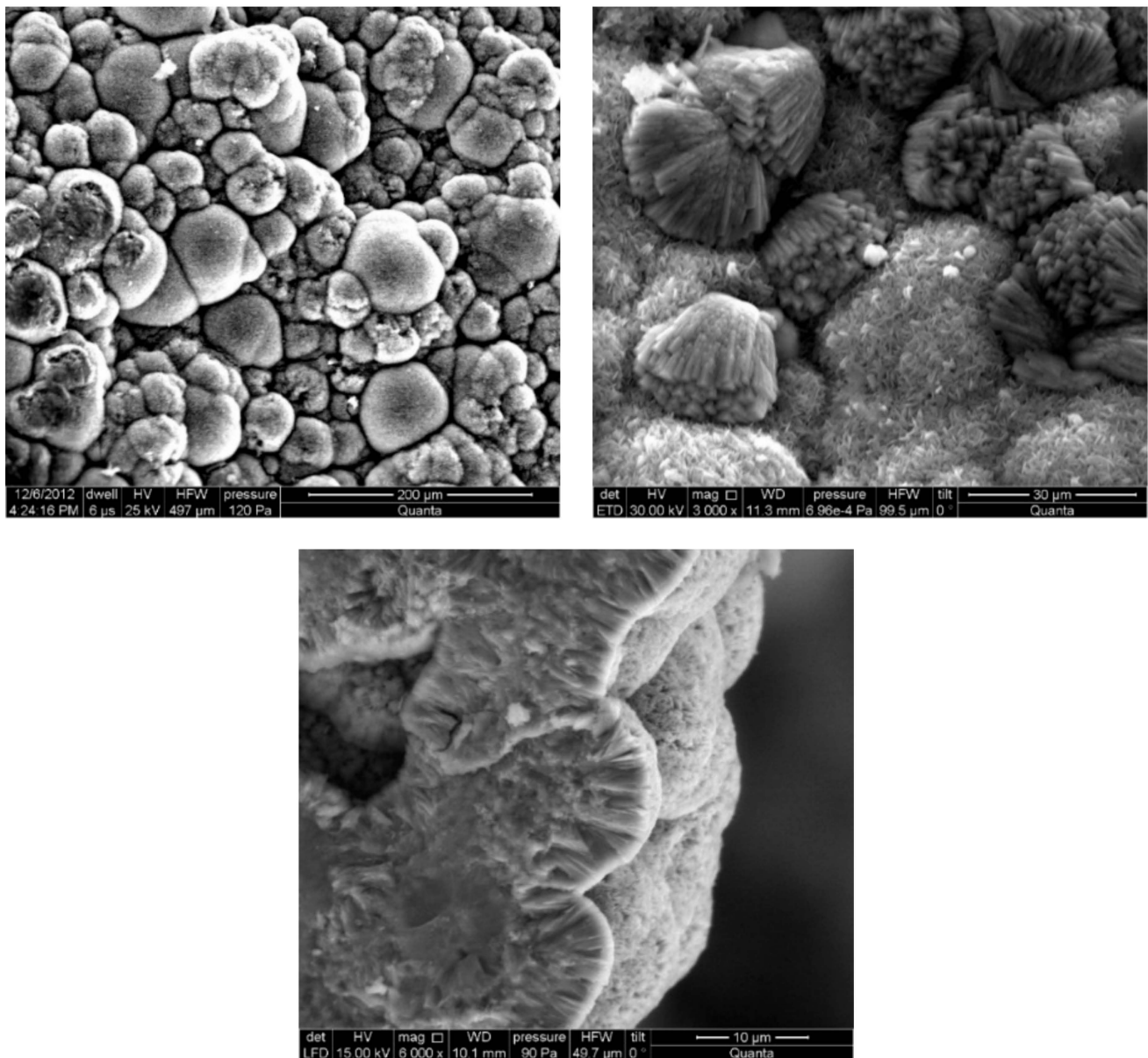
Figure 8. Microphotographs of corrosion scale, which forms a dry layer of the metal base of the pipe.

4. Conclusions

The corrosion in water-supplying steel pipes with the formation of fistulas, as a rule, proceeds in several stages. The results of the study propose a corrosion model that considers the entire process as a whole. In the first stage, ulcerative corrosion develops, accompanied by the growth of tubercles covered with a dense layer of corrosion products (magnetite). In subsequent stages, corrosion develops by a pitting mechanism inside the tubercles. The emergence of fistulas is preceded by an increase in the concentration of electrolyte inside the tubercles due to the peculiarities of the structure of the dense layer. Within the formation, the dense layer acquires the properties of a selective membrane.

An increase in the concentration of electrolyte on the metal surface under a tubercle intensifies the pitting corrosion, converting unstable pits into stable ones. At the final stage, the growth of tubercles ceases, and the process becomes autocatalytic. In this case, the presence of sufficient water within the core of the tubercle provides conditions for the formation of a fistula. If there is no external water supply, fistulas may form only if there is sufficient water in the tubercular structure to oxidize the entire iron, considering the thickness of the remaining metal. In the pits, water is consumed by the hydrolysis of

iron liberated during corrosion. In cases of water scarcity, individual pits and, generally, tubercles become repassivated. Consequently, pipes with thicker walls, such as cast iron, are more resistant to corrosion. It is proposed that the dense layer in the tubercles in carbon steels and the perforated coating in the structure of the pitting in stainless steels have identical properties, ensuring the creation of critical conditions for intense corrosion.

The studies carried out to determine the concentration of salts in the structure of the tubercles after extraction from pipes can be used to better understand the mechanism of corrosion. At the same time, it is necessary to study not only the structure but also the properties of the dense layer, which will allow the determination of the directions of influence on the ongoing corrosion processes.

The results of the research propose a new direction to assess the influence of a dense layer on the corrosion of steel and cast-iron pipes before the appearance of fistulas. A possible change in the electrical resistance of the layer when applying various inhibitors is also presented.

Author Contributions: Conceptualization, V.C., A.A. and N.M.; methodology, V.C., A.A. and N.M.; software, N.M.; validation, V.C. and A.A.; formal analysis, V.C., A.A. and N.M.; investigation, V.C., A.A. and N.M.; resources, V.C., A.A. and N.M.; data curation, V.C. and A.A.; writing—original draft preparation, V.C. and A.A.; writing—review and editing, N.M.; visualization, N.M. and V.C.; supervision, N.M.; project administration, N.M.; funding acquisition, N.M. All authors have read and agreed to the published version of the manuscript.

Institutional Review Board Statement: Not applicable.

Informed Consent Statement: Not applicable.

Data Availability Statement: The original contributions presented in the study are included in the article, further inquiries can be directed to the corresponding author.

Conflicts of Interest: The authors declare no conflicts of interest.

References

1. Kosygin, A.B.; Fomina, I.V.; Goritsky, V.M.; Khromov, D.P. Methodology of assessment of the technical condition and residual life of pipelines of water supply and sewerage networks in Moscow. *Water Supply Sanit. Tech.* **2010**, *3*, 31–36.
2. Sander, A.; Berghult, B.; Elfstroem Broo, A.; Lind Johansson, E.; Hedberg, T. Iron corrosion in drinking water distribution systems—The effect of pH, calcium and hydrogen carbonate. *Corrosion Sci.* **1996**, *38*, 443–455. [CrossRef]
3. Su, P.; Fuller, D.B. *Corrosion and Corrosion Mitigation in Fire Protection Systems*, 2nd ed.; Project ID 0003040794; FM Global: Norwood, MA, USA, 2014.
4. Delaunois, F.; Tosar, F.; Vitry, V. Corrosion behaviour and biocorrosion of galvanized steel water distribution systems. *Bioelectrochemistry* **2014**, *97*, 110–119. [CrossRef] [PubMed]
5. Marjanowski, J.; Ostrowski, J. *Electrochemical Protection against Corrosion Processes in Hot Tap Water Installations*; C.B.W. UNITEX Ltd.: Gdansk, Poland, 2015.
6. Clarke, B.H.; Aguilera, A.M. *Microbiologically Influenced Corrosion in Fire Sprinkler Systems Automatic Sprinkler Systems, Handbook*; National Fire Protection Association: Quincy, MA, USA, 2007.
7. Chukhin, V.A.; Andrianov, A.P. Formation mechanism of iron tubercles during corrosion of water supply pipes. *Int. J. Corros. Scale Inhib.* **2022**, *11*, 812–830. [CrossRef]
8. Zhong, H.; Tang, Y.; Yan, H.; Zhang, Y.; Dong, L.; Wang, B. Corrosion of pipelines in urban water systems: Current research status and future trends based on bibliometric analysis. *J. Water Process Eng.* **2023**, *56*, 104288. [CrossRef]
9. Edwards, M.; Arnold, R.; Rosenfeldt, B.; Masters, S.V.; Parks, J.; Tang, M. Utility considerations in developing a galvanized iron water pipe management plan. *AWWA Water Sci.* **2023**, *5*, e1350. [CrossRef]
10. Ray, R.I.; Lee, J.S.; Little, B.J.; Gerke, T. The anatomy of tubercles: A corrosion study in a fresh water estuary. *Mater. Corros.* **2010**, *61*, 993–999. [CrossRef]
11. Herro, H.M. MIC myths—Does pitting cause MIC? In Proceedings of the Corrosion 98, San Diego, CA, USA, 22–27 March 1998. Paper No. 278.
12. Zhao, L.; Liu, D.; Zhang, H.; Wang, J.; Zhang, X.; Liu, S.; Chen, C. Study on electrochemical reduction mechanisms of iron oxides in pipe scale in drinking water distribution system. *Water Res.* **2023**, *231*, 119597. [CrossRef]

13. Durrani, F.; Wesley, R.; Srikandarajah, V.; Eftekhari, M.; Munn, S. Predicting Corrosion rate in Chilled HVAC Pipe Network: Coupon vs Linear Polarisation Resistance method. *Eng. Fail. Anal.* **2020**, *109*, 104261. [CrossRef]

14. Sarin, P.; Snoeyink, V.; Lytle, D.; Kriven, W. Iron corrosion scales: Model for scale growth, iron release, and colored water formation. *J. Environ. Eng.* **2004**, *30*, 364–373. [CrossRef]

15. Martins, C.M.B.; Moreira, J.L.; Martins, J.I. Corrosion in water supply pipe stainless steel 304 and a supply line of helium in stainless steel 316. *Eng. Fail. Anal.* **2014**, *39*, 65–71. [CrossRef]

16. Li, Z.H.; Han, Y.M.; Zhao, Y.G.; Yang, S.L.; Zhong, Z.M.; Lu, Y.H. Thermal corrosion fatigue crack growth behavior and life prediction of 304SS pipeline structures in high temperature pressurized water. *Eng. Fail. Anal.* **2024**, *160*, 108224. [CrossRef]

17. Farh, H.M.H.; Seghier, M.E.A.B.; Zayed, T. A comprehensive review of corrosion protection and control techniques for metallic pipelines. *Eng. Fail. Anal.* **2023**, *143*, 106885. [CrossRef]

18. Swietlik, J.; Raczyk-Stanisławiak, U.; Piszora, P.; Nawrocki, J. Corrosion in drinking water pipes: The importance of green rusts. *Water Res.* **2012**, *46*, 1–10. [CrossRef] [PubMed]

19. Tong, H.; Zhao, P.; Zhang, H.; Tian, Y.; Chen, X.; Zhao, W.; Li, M. Identification and characterization of steady and occluded water in drinking water distribution systems. *Chemosphere* **2015**, *119*, 1141–1147. [CrossRef] [PubMed]

20. Smith, F.; Brownlie, F.; Hodgkiess, T.; Toumpis, A.; Pearson, A.; Galloway, A.M. Effect of salinity on the corrosive wear behaviour of engineering steels in aqueous solutions. *Wear* **2020**, *462–463*, 203515. [CrossRef]

21. Nawrocki, J.; Raczyk-Stanisławiak, U.; Świetlik, J.; Olejnik, A.; Sroka, M.J. Corrosion in a distribution system: Steady water and its composition. *Water Res.* **2010**, *44*, 1863–1872. [CrossRef]

22. Abdalsamed, I.; Amar, I.; Sharif, A.; Ghnim, M.; Farouj, A.; Kawan, J. Scale Corrosion of Metallic Materials in Water Systems—A Review. *J. Chem. Rev.* **2022**, *4*, 67–80. [CrossRef]

23. Soltis, J.; Krouse, D.; Laycock, N. Localized dissolution of iron in buffered and non-buffered chloride containing solutions. *Corros. Sci.* **2011**, *53*, 2152–2160. [CrossRef]

24. Hu, J.; Dong, H.; Xu, Q.; Ling, W.; Qu, J.; Qiang, Z. Impacts of water quality on the corrosion of cast iron pipes for water distribution and proposed source water switch strategy. *Water Res.* **2018**, *129*, 428–435. [CrossRef]

25. Soltis, J. Passivity breakdown, pit initiation and propagation of pits in metallic materials—Review. *Corros. Sci.* **2015**, *90*, 5–22. [CrossRef]

26. Galvele, J.R. Transport processes in passivity breakdown—II. Full hydrolysis of the metal ions. *Corros. Sci.* **1981**, *21*, 551–579. [CrossRef]

27. Pistorius, P.C.; Burstein, G.T. Metastable pitting corrosion of stainless steel and the transition to stability. *Philosoph. Transact. A* **1992**, *341*, 531–559. [CrossRef]

28. Gaudet, G.T.; Mo, W.T.; Hatton, T.A.; Tester, J.W.; Tilly, J.; Isaacs, H.S.; Newman, R.C. Mass transfer and electrochemical kinetic interactions in localized pitting corrosion. *AIChE J.* **1986**, *32*, 949–958. [CrossRef]

29. Pistorius, P.C.; Burstein, G.T. Growth of corrosion pits on stainless steel in chloride solution containing dilute sulphate. *Corros. Sci.* **1992**, *33*, 1885–1897. [CrossRef]

30. Scheiner, S.; Hellmich, C. Stable pitting corrosion of stainless steel as diffusion-controlled dissolution process with a sharp moving electrode boundary. *Corrosion Sci.* **2007**, *49*, 319–346. [CrossRef]

31. Heurtault, S.; Robin, R.; Rouillard, F.; Vivier, V. On the propagation of open and covered pit in 316l stainless steel. *Electrochim. Acta* **2016**, *203*, 316–325. [CrossRef]

32. Lin, H.; Hu, Y. Impact of different source-water switching patterns on the stability of drinking water in an estuarine urban water distribution system. *Environ. Sci. Pollut Res.* **2022**, *29*, 49059–49069. [CrossRef] [PubMed]

33. Burstein, G.T.; Liu, C.; Souto, R.M.; Vines, S.P. Origins of pitting corrosion. *Corrosion Eng. Sci. Technol.* **2004**, *39*, 25–30. [CrossRef]

34. Heurtault, S.; Robin, R.; Rouillard, F.; Vivier, V. Initiation and propagation of a single pit on stainless steel using a local probe technique. *Faraday Discuss.* **2015**, *180*, 267–282. [CrossRef]

35. Frankel, G.S. Pitting corrosion of metals. A review of the critical factors. *J. Electrochem. Soc.* **1998**, *145*, 2186–2198. [CrossRef]

36. Li, K.; Sun, L.; Cao, W.; Chen, S.; Chen, Z.; Wang, Y.; Li, W. Pitting corrosion of 304 stainless steel in secondary water supply system. *Corros. Commun.* **2022**, *7*, 43–50. [CrossRef]

37. Subramanian, C. Localized pitting corrosion of API 5L grade A pipe used in industrial fire water piping applications. *Eng. Fail. Anal.* **2018**, *92*, 405–417. [CrossRef]

38. Wong, K.P.; Alkire, R.C. Local Chemistry and Growth of Single Corrosion Pits in Aluminum. *J. Electrochem. Soc.* **1990**, *137*, 3010–3015. [CrossRef]

39. Beck, T.R. Formation of Salt Films during Passivation of Iron. *J. Electrochem. Soc.* **1982**, *129*, 2412–2418. [CrossRef]

40. Rudnicka, Ł.; Swiderska-Broz, M. Chemical composition of deposits in Wroclaw distribution system. *Ochrona Srodowiska* **1995**, *58*, 63–65.

41. Fabbricino, M.; Korshin, G.V. Changes of the corrosion potential of iron in stagnation and flow conditions and their relationship with metal release. *Water Res.* **2014**, *62*, 136–146. [CrossRef] [PubMed]

42. Al Ameri, M.; Yi, Y.; Cho, P.; Al Saadi, S.; Jang, C.; Beeley, P. Critical conditions for pit initiation and growth of austenitic stainless steels. *Corros. Sci.* **2015**, *92*, 209–216. [CrossRef]

43. Chukhin, V.A.; Andrianov, A.P. The Wave Nature of Tubercle Corrosion in Steel and Cast Iron Pipes of Water Supply Systems. *Vestnik MGSU* **2018**, *13*, 385–399. [CrossRef]

44. Tsunoda, Y. Electrodialysis for producing brine concentrates seawater. In Proceedings of the First International Symposium on Water Desalination, Washington, DC, USA, 3–9 October 1965. SWD/31.

45. Garza, G.; Kedem, O. Electroosmotic pumping in unit cells. In Proceedings of the 5th International Symposium on Fresh Water from the Sea, Alghero, Italy, 16–20 May 1976; Volume 3, pp. 79–87.

46. Smagin, V.N.; Chukhin, V.A.; Kharchuck, V.A. Technological account of electrodialysis apparatus for concentration. *Desalination* **1983**, *46*, 283–290. [CrossRef]

47. El Wanees, S.A.; Kamel, M.M.; Rashwan, S.M.; Atef, Y.; Abd El Sadek, M.G. Initiation and inhibition of pitting corrosion on C-steel in oilfield-produced water under natural corrosion conditions. *Desalin. Water Treat.* **2022**, *248*, 28–38. [CrossRef]

48. Ergun, M.; Turan, A.Y. Pitting potential and protection potential of carbon steel for chloride ion and the effectiveness of different inhibiting anions. *Corros. Sci.* **1991**, *32*, 1137–1142. [CrossRef]

49. Zhang, S.; Wang, Y.; Li, S.; Wang, Z.; Chen, H.; Yi, L.; Chen, X.; Yang, Q.; Xu, W.; Wang, A.; et al. Concerning the stability of seawater electrolysis: A corrosion mechanism study of halide on Ni-based anode. *Nat. Commun.* **2023**, *14*, 4822. [CrossRef] [PubMed]